Ultrasound in Med. & Biol., Vol. 35, No. 1, pp. 129–135, 2009

0301-5629/09/$–see front matter

ELSEVIER

doi:10.1016/j.ultrasmedbio.2008.06.006

● *Original Contribution*

THRESHOLD ESTIMATION AND SUPERTHRESHOLD BEHAVIOR OF ULTRASOUND-INDUCED LUNG HEMORRHAGE IN RATS: ROLE OF AGE DEPENDENCY

WILLIAM D. O'BRIEN, JR.,* YAN YANG,† and DOUGLAS G. SIMPSON‡

*Bioacoustics Research Laboratory, Department of Electrical and Computer Engineering, University of Illinois, Urbana, IL, USA; †Department of Mathematics and Statistics, Arizona State University, Tempe, AZ, USA; and ‡Department of Statistics, University of Illinois, Champaign, IL, USA

(*Received* 7 *March* 2008; *revised* 27 *May* 2008; *in final form* 16 *June* 2008)

Abstract—Age-dependent threshold and superthreshold behaviors of ultrasound-induced lung hemorrhage were investigated with one hundred ten 12.6 ± 0.8-d-old rats, one hundred ten 22.9 ± 0.8-d-old rats, and one hundred 57.7 ± 3.9-d-old rats. Exposure conditions were: 2.8 MHz, 10-s exposure duration, 1-kHz pulse repetition frequency and 1.3-μs pulse duration. The *in situ* (at the pleural surface) peak rarefactional pressure ($p_{r(in\ situ)}$) ranged between 1.4 and 10.8 MPa for which there were either 9 or 10 acoustic pressure groups for each of the three rat ages (10 rats/exposure group). For each of the three rat ages there were also shams; there were no lesions in the shams. The $p_{r(in\ situ)}$ levels were randomized within each age group; rat age was not randomized. Individuals involved in animal handling, exposure and lesion scoring were blinded to the exposure condition. In addition, one hundred fifty-six 72-d-old rats were included from three completed studies (same experimental conditions) to provide a fourth age group for the analysis. Probit regression analysis was used to examine the dependence of the occurrence of lesions on $p_{r(in\ situ)}$ in the four age groups. Likewise, lesion depth and lesion root surface area were analyzed using Gaussian tobit regression analysis. Although $p_{r(in\ situ)}$ was a significant variable, no significant age dependence of the $p_{r(in\ situ)}$ effect was found. Furthermore, age had no significant effect on either the rate of occurrence or the depth of lesions. Given the occurrence of a lesion, a weak age dependence was found for the median surface area of the induced lesion (p-value = 0.037). (E-mail: wdo@uiuc.edu)

Key Words: **Lung, Pulmonary hemorrhage, Pulsed ultrasound, Rat.**

INTRODUCTION

The study reported herein evaluates one of the risk factors for ultrasound-induced lung hemorrhage, that is, age dependency because there have been several conflicting observations. These conflicting observations have been summarized previously (O'Brien et al. 2003a). Briefly, monkey studies suggested that younger animals had a greater likelihood for ultrasound-induced lung hemorrhage compared with older animals (Tarantal and Canfield 1994). Mice were reported to have an age-independent ultrasound-induced lung-hemorrhage threshold (Dalecki et al. 1997a). Also, one research group reported that neonate (1-d-old) (Baggs et al. 1996) and young (10-d-old) pigs had an age-independent lung-hemorrhage threshold (Dalecki et al. 1997b). However, when these younger (1- and 10-d-old) pig studies are compared with another pig study of older animals (10- to 12-wk-old) (O'Brien and Zachary 1997), younger pigs were more sensitive than the older pigs, that is, an age-dependent observation between separately conducted studies. And, age-dependent lung-hemorrhage thresholds were reported with middle-aged (39-d-old) pigs being least susceptible to lung damage, oldest (58-d-old) pigs being most susceptible to lung damage and neonate (4.9-d-old) pigs having intermediate susceptibility to lung damage (O'Brien et al. 2003a).

Three species (mouse, pig, and monkey) have been investigated but the age dependencies of ultrasound-induced lung hemorrhage in rats have not. Therefore, the study reported herein estimated the *in situ* peak rarefactional pressure threshold levels and the sensitivity to lung damage at superthreshold exposure conditions in Sprague Dawley rats at three ages (12.6 ± 0.8-d-, 22.9 ±

Address correspondence to: William D. O'Brien, Jr., Bioacoustics Research Laboratory, Department of Electrical and Computer Engineering, University of Illinois, 405 N. Mathews, Urbana, IL 61801. E- mail: wdo@uiuc.edu

0.8-d-, 57.7 ± 3.9-d-old). In addition, a fourth age group (72-d-old) was included for the age-dependent ultrasound-induced lung hemorrhage analysis from a compilation of three completed rat studies (Zachary et al. 2001; O'Brien et al. 2001, 2003b) for which the same experimental conditions were used.

MATERIALS AND METHODS

Animals

The experimental protocol was approved by the Institutional Animal Care and Use Committee (IACUC) of the University of Illinois and satisfied all campus and National Institutes of Health rules for the humane use of laboratory animals. Animals were housed in an Association for Assessment and Accreditation of Laboratory Animal Care (AAALAC), Rockville, MD -approved animal facility and provided food and water *ad libitum*.

There were a total of one hundred ten 12.6 ± 0.8-d-old (mean ± SD) rats (weight: 26.7 ± 3.6 g; chest wall thickness: 1.6 ± 0.2 mm), one hundred ten 22.9 ± 0.8-d-old rats (weight: 53.4 ± 6.6 g; chest wall thickness: 1.8 ± 0.1 mm), and one hundred 57.7 ± 3.9-d-old rats (weight: 235 ± 48 g; chest wall thickness: 3.8 ± 0.5 mm). All Sprague Dawley rats were obtained from Harlan (Indianapolis, IN, USA). These three age groups will also be referred to as 13-d-, 23-d- and 58-d- rats for convenience. Animal weights were measured at the time of the experiment and animal ages were determined from exact birth date. The selection of these age (weight) groups was somewhat arbitrary because the mechanisms by which ultrasound produces lung hemorrhage are not understood and, thus, the selection could not have a specific biological basis. Nevertheless, there are maturation changes as the animal ages, particularly those based on recognized rat time points. These time points are linked to biological events. Such categories include preweaned rats (13-d-old group), postweaned rats (23-d-old group) and adult rats (58-d-old group).

In each age group, rats were assigned randomly to 11 (13 d and 23 d) or 10 (58 d) acoustic pressure levels (Table 1), each with 10 rats/pressure level. Pulsed ultrasound exposure conditions were: 2.8 MHz, 10-s exposure duration, 1-kHz pulse repetition frequency and 1.3-μs pulse duration. No lesions were produced in the sham exposed rats. The individuals involved in rat handling, exposure, necropsy and lesion scoring were blinded to the exposure condition. The exposure condition for each rat was revealed only after the final results were tabulated.

In addition, a fourth age group (156 72-d-old rats) was included for the age-dependent ultrasound-induced lung hemorrhage analysis from a compilation of three completed studies (Zachary et al. 2001; O'Brien et al. 2001, 2003b) for which the same experimental conditions were used.

Rats were weighed and then anesthetized with ketamine hydrochloride (87.0 mg/kg) and xylazine (13.0 mg/kg) administered intraperitoneally. Hair of the left thorax was removed with an electric clipper, followed by a depilatory agent (Nair® Carter-Wallace, Inc., New York, NY, USA) to maximize sound transmission. A black dot was placed at approximately the sixth to ninth rib to guide the positioning of the ultrasonic beam. Anesthetized animals were placed in a specially designed transducer holder. A removable pointer, attached to the transducer, was used to position the ultrasonic beam perpendicular to the skin at the position of the black dot with the beam's focal region approximately at the lung surface. The holder with animal and mounted transducer was placed in highly degassed, temperature-controlled (30°C) water. In pulse-echo mode, the low-power output signal (see shams in Table 1) from the RAM5000 (Ritec, Inc., Warwick, RI, USA) was displayed on an oscilloscope and used to adjust the axial center of the focal region to within 1 mm of the lung surface. Following exposure, animals were removed from the water and holder, and then euthanized under anesthesia by cervical dislocation.

The thorax was opened and the thickness of each left thoracic wall (skin, rib cage and parietal pleura) was measured using a digital micrometer (accuracy: 10 μm; Mitutoyo Corp., Kawasaki, Kanagawa, Japan) to calculate the *in situ* peak rarefactional pressure. The left lung lobe was scored for the presence or absence of hemorrhage and then fixed by immersion in 10% neutral-buffered formalin for a minimum of 24 h. After fixation, the elliptical dimensions of each lung lesion at the visceral pleural surface were measured using a digital micrometer where "a" is the semi-major axis and "b" is the semi-minor axis. The lesion was then bisected and the depth "d" of the lesion within the pulmonary parenchyma was also measured. The surface area (πab) of the lesion was calculated for each animal. Each half of the bisected lesion was embedded in paraffin, sectioned at 5 μm, stained with hematoxylin and eosin and evaluated microscopically.

Exposimetry

The exposimetry and calibration procedures have been described previously in detail (Zachary et al. 2001). Ultrasonic exposures were conducted using a focused f/1 19-mm-diameter, lithium niobate ultrasonic transducer (Valpey Fisher, Hopkinton, MA, USA). Water-based (highly degassed water, 22°C) pulse-echo ultrasonic field distribution measurements were performed according to established procedures (Raum and O'Brien 1997) and

Table 1. Mean age, mean (SEM) values of the *in situ* (at the pleural surface) peak rarefactional pressure $p_{r(in\ situ)}$ and *in situ* peak compressional pressure $p_{c(in\ situ)}$ and their respective lesion occurrence and mean (SEM) values of the lesion depth and surface area

Mean age (d)	$p_{r(in\ situ)}$ (SEM) (MPa)	$p_{c(in\ situ)}$ (SEM) (MPa)	Mechanical index	% lesion occurrence (uncertainty)	Mean (SEM) lesion depth (mm)	Mean (SEM) lesion area (mm^2)
13-d rats (10 rats per group)						
13.1 (sham)	0.37 (0.001)	0.45 (0.001)	0.18	0	–	–
12.9	1.4 (0.002)	1.3 (0.002)	0.68	0	–	–
12.5	2.2 (0.002)	2.2 (0.002)	1.1	0	–	–
12.9	2.9 (0.004)	2.9 (0.005)	1.4	0	–	–
12.7	3.7 (0.008)	3.9 (0.009)	1.8	30 (14)	0.50 (0.27)	1.08 (0.67)
12.3	4.4 (0.007)	4.7 (0.007)	2.2	0	–	–
12.8	5.3 (0.008)	5.6 (0.009)	2.6	30 (14)	0.18 (0.14)	0.30 (0.26)
12.5	6.5 (0.006)	7.5 (0.007)	3.2	30 (14)	0.11 (0.07)	0.11 (0.07)
12.3	8.4 (0.013)	9.7 (0.015)	4.1	60 (15)	0.37 (0.13)	0.75 (0.23)
12.2	9.2 (0.005)	11.3 (0.006)	4.7	60 (15)	0.37 (0.15)	0.16 (0.21)
12.7	10.3 (0.006)	12.9 (0.008)	5.2	60 (15)	0.36 (0.12)	0.48 (0.15)
23-d rats (10 rats per group)						
22.6 (sham)	0.37 (0.000)	0.45 (0.000)	0.18	0	–	–
23.0	2.9 (0.003)	2.9 (0.003)	1.4	0	–	–
23.1	3.7 (0.002)	3.9 (0.002)	1.8	10 (9)	0.02 (0.02)	0.07 (0.07)
23.2	4.6 (0.004)	4.9 (0.004)	2.3	20 (13)	0.07 (0.06)	0.11 (0.09)
23.0	5.5 (0.005)	6.1 (0.005)	2.8	30 (14)	0.29 (0.15)	0.36 (0.19)
23.0	6.4 (0.005)	7.4 (0.006)	3.2	40 (15)	0.35 (0.18)	0.67 (0.35)
23.2	7.2 (0.005)	7.7 (0.005)	3.6	50 (16)	0.54 (0.19)	1.59 (0.55)
23.3	7.7 (0.007)	8.9 (0.008)	3.8	70 (14)	0.70 (0.17)	1.34 (0.37)
22.0	8.6 (0.007)	10.1 (0.008)	4.3	60 (15)	0.54 (0.20)	1.09 (0.40)
23.0	9.2 (0.005)	11.2 (0.007)	4.7	90 (9)	0.96 (0.18)	1.99 (0.45)
22.8	10.3 (0.009)	12.9 (0.011)	5.2	90 (9)	0.87 (0.21)	1.68 (0.49)
58-d rats (10 rats per group)						
56.9 (sham)	0.34 (0.002)	0.42 (0.003)	0.18	0	–	–
59.9	4.9 (0.028)	5.2 (0.030)	2.6	0	–	–
53.8	5.1 (0.026)	5.7 (0.028)	2.8	20 (13)	0.37 (0.28)	0.89 (0.83)
58.9	5.6 (0.029)	6.0 (0.031)	3.1	30 (14)	0.34 (0.19)	0.70 (0.36)
58.2	6.7 (0.034)	7.2 (0.036)	3.6	30 (14)	0.52 (0.27)	1.23 (0.73)
58.7	7.8 (0.041)	9.0 (0.047)	4.1	60 (15)	0.37 (0.14)	0.75 (0.44)
57.9	8.7 (0.049)	10.6 (0.060)	4.7	50 (16)	0.50 (0.22)	0.81 (0.45)
59.9	9.7 (0.052)	12.2 (0.065)	5.2	50 (16)	0.60 (0.22)	2.03 (1.00)
53.7	10.3 (0.059)	13.9 (0.079)	5.5	90 (9)	1.6 (0.31)	5.33 (2.08)
59.2	10.8 (0.058)	15.1 (0.081)	5.7	80 (13)	1.4 (0.31)	5.26 (1.31)

All rats were exposed to pulsed ultrasound (1-kHz PRF, 10-s ED, 1.3-μs PD). The sham exposure conditions used a pulse repetition frequency of 10 Hz. Mean values of the mechanical index (MI), as measured according to the applicable standard (ODS 1998), are provided because the MI is a regulated quantity of diagnostic ultrasound equipment.

yielded a center frequency of 2.8 MHz, a fractional bandwidth of 12%, a focal length of 19 mm, a −6-dB focal beamwidth of 470 μm and a −6-dB depth of focus of 2.7 mm. Ultrasound-induced lesions at superthreshold levels have generally been larger in diameter than the reported −6-dB focal beamwidth (O'Brien et al. 2001) because (1) there is lung motion as the animal breaths and (2) as $p_{r(in\ situ)}$ increases above threshold, more of the beam incident on the lung surface is involved in producing damage. The reported water-based pulse-echo −6-dB focal beamwidth is provided for transducer/beam characterization purposes only (*e.g.,* −40-dB focal beamwidth is 1 mm).

An automated procedure, based on established standards (ODS 1998; AIUM/NEMA 1998), was used to routinely calibrate the ultrasound fields (Sempsrott and O'Brien 1999; Zachary et al. 2001). Briefly, the source transducer's drive voltage was supplied by a RAM 5000. A calibrated PVDF membrane hydrophone (Marconi Model Y-34-6543, Chelmsford, UK) was mounted to the computer-controlled micropositioning system (Daedal, Inc., Harrisburg, PA, USA). The hydrophone's signal was digitized (500 MS/s, LeCroy model 9354TM Oscilloscope, Chestnut Ridge, NY, USA), the output of which was fed to the same computer (Dell Pentium II, Dell Corporation, Round Rock, TX, USA) that controlled the positioning system. Off-line processing (Matlab, The Mathworks, Natick, MA, USA) yielded the water-based peak rarefactional pressure $p_{r(in\ vitro)}$ and the water-based peak compressional pressure $p_{c(in\ vitro)}$. The mechanical

index (MI) was also determined from the measurement procedure (ODS 1998); the MI = $p_{r.3}/\sqrt{f_c}$ where $p_{r.3}$ is the computationally derated (0.3 dB/cm-MHz) peak rarefactional pressure (in MPa) and f_c is the center frequency (in MHz). The MI is reported because it is a regulated quantity (FDA 1997) of diagnostic ultrasound systems and its value is available to system operators. Thus, there is value to provide the MI for each exposure setting in order to give general guidance to manufacturers and operators as to the exposure levels used in this study. Further, as seen from the MI definition, it is a quantity that must be determined from the water-based measurement process, and cannot be determined from the *in situ* (at the pleural surface) peak rarefactional pressure, $p_{r(in\ situ)}$. The study herein did not use the MI as a design variable; rather the $p_{r(in\ situ)}$ was the principal design variable.

A total of 14 independent water-based calibrations of the 2.8-MHz transducer were conducted before, during, and after the 4-month period of the experiments. At the exposure levels used in this study, the relative standard deviation (SD x 100/mean) was 6% for $p_{r(in\ vitro)}$ and 8% for $p_{c(in\ vitro)}$.

The *in situ* (at the pleural surface) peak rarefactional and compressional pressures ($p_{r(in\ situ)}$ and $p_{c(in\ situ)}$, respectively; Table 1) were estimated, as has been done in previous studies (Zachary et al. 2001) for each rat, using the mean attenuation coefficient at 2.8 MHz of 2.8 dB/cm (Teotico et al. 2001; Towa et al. 2002) and the individually measured intercostal tissue thicknesses.

Statistical analysis

The primary interest in this analysis was to assess the combined effect of an animal's age and $p_{r(in\ situ)}$ on the occurrence, depth and surface area of lesions in exposed lungs. Probit regression analysis and tobit regression analysis were used to assess the significance of the age and $p_{r(in\ situ)}$ effects. The effective dose (ED) thresholds corresponding to 5% and 50% risk levels are termed, respectively, ED_{05} and ED_{50} (O'Brien et al. 2001, 2003a, 2003b, 2006; Simpson et al. 2004).

The lesion occurrence data were modeled by probit regression analysis, with age-dependent models of the form

$$\Pr(Y > 0) = \Phi(\beta_{a0} + \beta_{a1}x), \quad a = 1, 2, 3, 4, \qquad (1)$$

where x is $p_{r(in\ situ)}$ in megapascals (MPa); the index a = 1, 2, 3 or 4 refers to one of the four age groups: (1) 12 to 14 d; (2) 22 to 24 d; (3) 53 to 62 d and (4) 72 d; Y denotes the size of a lesion so $Y > 0$ denotes that a lesion is detected whereas $Y = 0$ denotes that no lesion is detected; and $\Phi(u) = (2\pi)^{-1/2}\int_{-\infty}^{u} e^{-x^2/2}dx$, the standard normal distribution function. Maximum likelihood estimates and standard errors for the coefficients β_{a0} and β_{a1} were computed from the occurrence data using the "glm" function in the R statistical programming language (Ihaka and Gentleman 1996; Hosmer and Lemeshow 2000).

To evaluate age and $p_{r(in\ situ)}$ effects on lesion occurrence, goodness-of-fit likelihood ratio statistics (*e.g.,* Hosmer and Lemeshow 2000) were computed for the following hypotheses versus the general alternative with eight unconstrained parameters. Below the hypotheses are ordered from least restrictive to most restrictive:

H_0 (No interaction between age and $p_{r(in\ situ)}$): $\beta_{11} = \ldots = \beta_{41}$

H_1 (No effect of age): $\beta_{10} = \ldots = \beta_{40}$; $\beta_{11} = \ldots = \beta_{41}$

H_2 (No age or $p_{r(in\ situ)}$ effect): $\beta_{10} = \ldots = \beta_{40}$; $\beta_{11} = \ldots = \beta_{41} = 0$

The hypotheses were tested for significance by comparing the corresponding likelihood ratio statistic for each hypothesis with the appropriate reference χ^2 distribution with degrees of freedom as indicated in Table 2. Note that if the computed p-value < 0.05, then the hypothesis is rejected at the significance level 0.05, otherwise it is accepted. If H_0 is rejected, for example, at the common significance level 0.05, then the conclusion is that there is a significant interaction between age and $p_{r(in\ situ)}$. If H_0 is accepted, then the effects of age and $p_{r(in\ situ)}$ are additive, in which case a likelihood ratio test is performed to determine if the main effect for age is significant. If H_1 is accepted, indicating the lack of any age effect, then testing hypothesis H_2 provides a check on whether the study has adequate power to detect the well-known $p_{r(in\ situ)}$ effect, as the vast previous literature strongly indicates an acoustic pressure effect.

Data on lesion depth and lesion surface area were modeled by tobit regression analysis. If a lesion occurred, then the measured depth and surface area were recorded. If no lesion occurred, then the lesion depth and surface area were recorded as zero values. Tobit regression analysis models these nonnegative-valued responses by treating 0 as a left-censoring point for Gaussian response data, that is, the model for the response Y, either depth (in mm) or square root of surface area (in mm), has the form

$$Y = \max(0, \gamma_{a0} + \gamma_{a1}x + \varepsilon), \quad a = 1, 2, 3, 4, \qquad (2)$$

where ϵ is a Gaussian noise variable with mean zero and standard deviation σ. Maximum likelihood estimates and standard errors for the parameters γ_{a0}, γ_{a1} and $\log(\sigma)$ were computed using the "survreg" function in R (Ihaka and Gentleman 1996; Galfalvy and Simpson 1999).

To evaluate age and acoustic pressure effects on lesion depth and surface area, likelihood ratio statistics were computed for the following hypotheses:

H_0* (No interaction between age and $p_{r(in\ situ)}$): $\gamma_{11} = \ldots = \gamma_{41}$

H_1* (No effect of age): $\gamma_{10} = \ldots = \gamma_{40}$; $\gamma_{11} = \ldots = \gamma_{41}$

H_2* (No age or $p_{r(in\ situ)}$ effect): $\gamma_{10} = \ldots = \gamma_{40}$; $\gamma_{11} = \ldots = \gamma_{41} = 0$

Goodness-of-fit likelihood ratio statistics were computed for these hypotheses to test for age and $p_{r(in\ situ)}$ effects. The goodness-of-fit statistics test each of these hypotheses against the general alternative model in which both the intercepts, γ_{a0}, and the $p_{r(in\ situ)}$ coefficients, γ_{a1}, depend on the age group.

The estimates for model 1 (eqn 1) and model 2 (eqn 2) were used to compute ED_{05} and ED_{50} thresholds and confidence intervals for these thresholds, as previously described (O'Brien et al. 2003a, 2003b; Simpson et al. 2004).

RESULTS

Chest wall thickness

The chest wall thickness over the left lung was measured for each rat. The mean ± SD (range) values of the chest wall thicknesses were: 1.6 ± 0.2 (1.3-1.9) mm (12 to 14 d, n = 110), 1.8 ± 0.1 (1.6-2.1) mm (22 to 24 d, n = 110), 3.8 ± 0.5 (3.2-4.6) mm (53 to 62 d, n to= 100), 4.6 ± 0.7 (3.3-6.0) mm (72-d, n = 156).

Lesion occurrence, depth and area

The ultrasound-induced lung hemorrhage results of rats as a function of age are shown in Fig. 1. The data from the three youngest age groups (12- to 14-d, 22- to 24-d and 53- to 62-d rats) were acquired for this study. The 72-d rat data were compiled from three separate studies (Zachary et al. 2001; O'Brien et al. 2001, 2003b) for which the experimental conditions were the same as used herein.

The statistical evidence for age and $p_{r(in\ situ)}$ effects on lesion occurrence is summarized in Table 2. The table presents goodness-of-fit likelihood ratio statistics for the models implied by hypotheses H_0, H_1 and H_2. The results indicate that H_0 and H_1 are accepted at the significance level 0.05, so there is no evidence of an age effect on occurrence of lesions, while H_3 is rejected, with a *p*-value less than 10^{-6}, so $p_{r(in\ situ)}$ is a highly significant factor and the test demonstrates a strong power in detecting it.

The statistical evidence for age and $p_{r(in\ situ)}$ effects on lesion depth is summarized in Table 3. The table presents goodness-of-fit likelihood ratio statistics of the hypotheses H_0*, H_1* and H_2* versus the general model of age-dependent baselines and $p_{r(in\ situ)}$ effects, based on tobit analysis of lesion depth. The results indicate that H_0* and H_1* are accepted, so there is no evidence of an age effect on lesion depth. The $p_{r(in\ situ)}$ effect was statistically significant, with a *p*-value less than 10^{-6}.

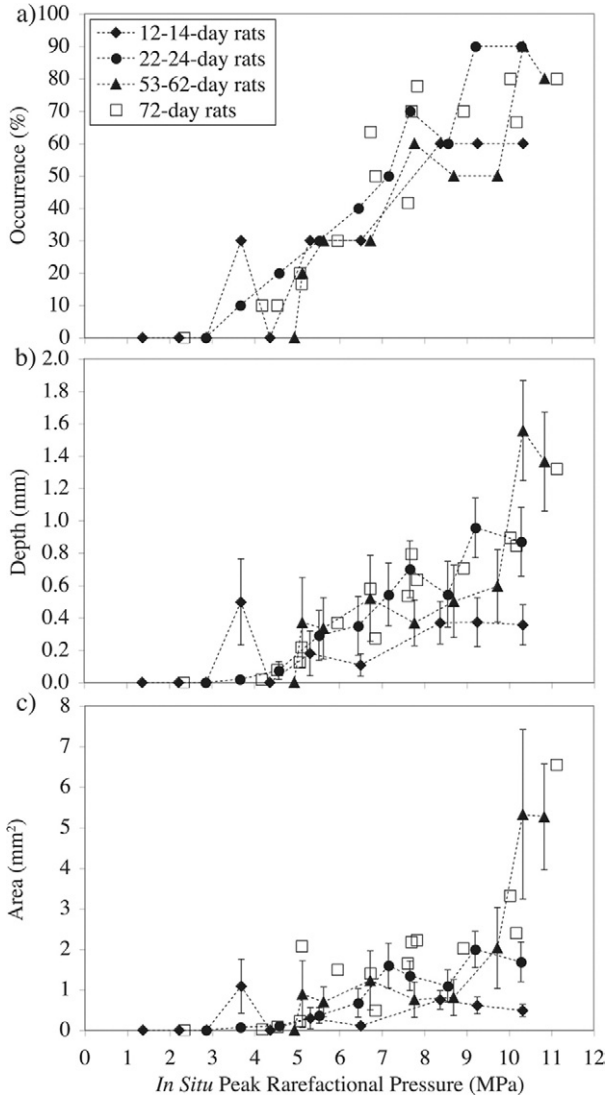

Fig. 1. (a) Lesion occurrence, (b) lesion depth and (c) lesion surface area as a function of the *in situ* peak rarefactional pressure. The dashed lines are straight lines connecting the mean values. The data from the three age groups (12-14-d, 22-24-d and 53-62-d rats) were acquired for this study. The 72-d rat data were compiled from three separate studies (Zachary et al. 2001; O'Brien et al. 2001, 2003b) for which the exposure conditions were the same as used herein, that is, 2.8-MHz center frequency, 1-kHz pulse repetition frequency, 10-s exposure duration and 470 μm beamwidth. Error bars are the standard errors of the mean (n = 10).

The statistical evidence for age and $p_{r(in\ situ)}$ effects on lesion surface area is summarized in Table 4. The table presents likelihood ratio tests of the hypotheses H_0*, H_1* and H_2* versus the general model of age-dependent baselines and $p_{r(in\ situ)}$ effects on lesion surface area, based on tobit regression analysis of the root-

Table 2. Goodness-of-fit likelihood ratio statistics for age and $p_{r(in\ situ)}$ effects on lesion occurrence based on probit regression models

Null hypothesis	−2 log-likelihood ratio	df	*p*-value
H_0: No age by $p_{r(in\ situ)}$ interaction	2.11	3	0.555
H_1: No age main effect	6.97	6	0.324
H_2: No age or $p_{r(in\ situ)}$ effect	145.4	7	$<10^{-6}$

In each case the alternative hypothesis is the full model with age-dependent intercepts and $p_{r(in\ situ)}$ coefficients.

Table 4. Goodness-of-fit likelihood ratio statistics for age and $p_{r(in\ situ)}$ effects on lesion surface area based on tobit regression models

Null hypothesis	−2 log-likelihood ratio	df	*p*-value
H_0*: No age by $p_{r(in\ situ)}$ interaction	3.70	3	0.295
H_0*: No age effect	12.21	6	0.057
H_0*: No age or $p_{r(in\ situ)}$ effect	166.5	7	$<10^{-6}$

In each case, the alternative hypothesis is the full model with age-dependent intercepts and $p_{r(in\ situ)}$ coefficients.

surface area. The interaction between age and $p_{r(in\ situ)}$ is not significant, so an additive model is appropriate. The near significance of the goodness-of-fit statistic for H_1* suggests a possible weak age dependence on the baseline surface area of lesions, given that they occur. This is confirmed by a likelihood ratio test of the age main effect, which gives a value of 12.21-3.70 = 8.51 on 3 degrees of freedom and a *p*-value = 0.0365.

Figure 2 displays 95% confidence intervals for ED_{05} and ED_{50} thresholds. These were derived from the full models that included age-dependent intercepts and $p_{r(in\ situ)}$ coefficients (eqn 1; eqn 2). ED_{05} thresholds are relevant for safety; ED_{50} thresholds are $p_{r(in\ situ)}$ levels at which 50% of the animals are expected to exhibit lesions. The figure is consistent with the lack of significant age differences among the ED_{05} (safety) thresholds, although there is some evidence for age variation among the ED_{50} thresholds derived from the lesion depth and surface area models.

DISCUSSION

The objective of this study was to assess the role of rat age on the threshold and superthreshold behaviors of ultrasound-induced lung hemorrhage because reports from previous findings (Tarantal and Canfield 1994; Baggs et al. 1996; Dalecki et al. 1997a, 1997b; O'Brien and Zachary 1997; O'Brien et al. 2003b) suggest that there was a lack of consistency observed relative to ultrasound-induced lung hemorrhage as a function of the animal's age.

There were no statistically significant age effects on occurrence or depth of lesions induced by focused ultrasound. There was some evidence of an age dependence of the lesion surface area given that a lesion had occurred, but no evidence that the $p_{r(in\ situ)}$ coefficient was dependent on age. Estimated thresholds were consistent with what has been found in other rat studies (Zachary et

Table 3. Goodness-of-fit likelihood ratio statistics for age and $p_{r(in\ situ)}$ effects on lesion depth based on tobit regression models

Null hypothesis	−2 log-likelihood ratio	df	*p*-value
H_0*: No age by $p_{r(in\ situ)}$ interaction	4.36	3	0.225
H_1*: No age effect	10.2	6	0.117
H_2*: No age or $p_{r(in\ situ)}$ effect	159.8	7	$<10^{-6}$

In each case the alternative hypothesis is the full model with age-dependent intercepts and $p_{r(in\ situ)}$ coefficients.

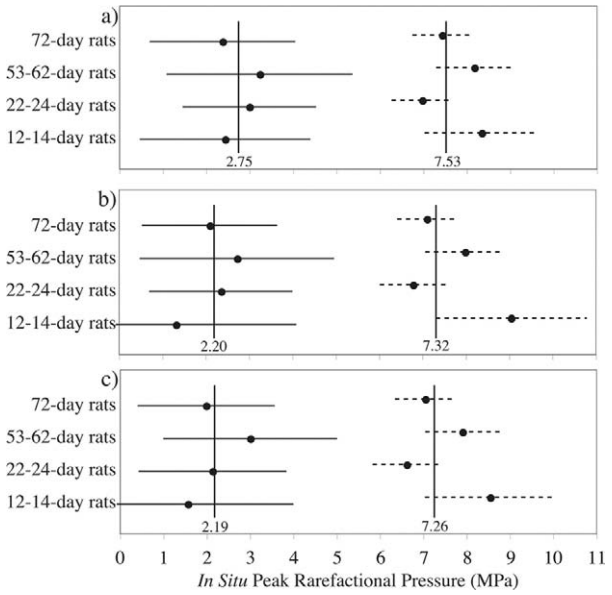

Fig. 2. Plots of 95% confidence intervals for the estimated ED_{05} (solid horizontal lines with the ED_{05} estimates located at the centers) and ED_{50} (dotted horizontal lines with the ED_{50} estimates located at the centers) based on (a) lesion occurrence, (b) lesion depth and (c) lesion area in rats. The x-axis indicates the *in situ* peak rarefactional pressure, and y-axis displays the rat age. The two vertical lines in each box represent the weighted averages of the ED_{05} and ED_{50} estimates, respectively, with the average values at the base of each vertical line. For each of the four studies, a common exposure regime was used: 2.8-MHz center frequency, 1-kHz pulse repetition frequency, 10-s exposure duration and 470-μm beamwidth.

al. 2001; O'Brien et al. 2001, 2003b). It is noteworthy that the strong age-dependence of thresholds found previously in pigs (O'Brien et al. 2003a) did not manifest itself in the present age-dependent threshold study in rats.

In summary, the conflicting observations remain. Four species have been investigated (mice, rats, pigs, monkeys). No age-dependent effect was reported in mice (Dalecki et al. 1997a). Age-dependent effects were reported in monkeys (Tarantal and Canfield 1994). Conflicting age-dependent effects were reported in pigs (Baggs et al. 1996; Dalecki et al. 1997b; O'Brien et al. 2003a). And, this study reported no age-dependent effect in rats. It is interesting to observe that no age-dependent effects have occurred in the two rodent models investigated, whereas to some extent, age-dependent effects occurred in monkeys and pigs. It is, thus, likely that age dependency of lung lesions is species dependent and the higher the animal is in the evolutionary chain, the more likely is such an effect. However, this latter comment is speculative and not able to be tested with the currently available data. Nevertheless, if it were true, then it is likely that ultrasound-induced lung hemorrhage thresholds would be age-dependent in humans, although the data do not suggest whether younger or older humans would be more susceptible to damage.

Acknowledgments—This work was supported by NIH Grant R37EB02641. The authors thank Dr. Rita J. Miller and James P. Blue, Jr. for technical experimental assistance.

REFERENCES

AIUM/NEMA, Acoustic Output Measurement Standard for Diagnostic Ultrasound Equipment. Laurel, MD, American Institute of Ultrasound in Medicine, and Rosslyn, VA, National Electrical Manufacturers Association, 1998.

Baggs R, Penney DP, Cox C, Child SZ, Raeman CH, Dalecki D, Carstensen EL. Thresholds for ultrasonically induced lung hemorrhage in neonatal swine. Ultrasound Med Biol 1996;22:119–128.

Dalecki D, Child SZ, Raeman CH, Raeman CH, Cox C, Penney DP, Carstensen EL. Age dependence of ultrasonically-induced lung hemorrhage in mice. Ultrasound Med Biol 1997a;23:767–776.

Dalecki D, Child SZ, Raeman CH, Cox C, Carstensen EL. Ultrasonically induced lung hemorrhage in young swine. Ultrasound Med Biol 1997b;23:777–781.

FDA, Information for Manufacturers Seeking Marketing Clearance of Diagnostic Ultrasound Systems and Transducers, Rockville, MD, Center for Devices and Radiological Health, US Food and Drug Administration, September 30, 1997.

Galfalvy H, Simpson DG. Infrastructure degradation: an application of censored regression models. In: American Statistical Association Proceedings of the Section on Physical and Engineering Sciences. Alexandria, VA: American Statistical Association; 1999:242–247.

Hosmer DW, Lemeshow S. Applied logistic regression, 2nd ed. New York: Wiley, 2000.

Ihaka R, Gentleman R. R: A language for data analysis and graphics. J Comput Graph Stat 1996;5:299–314.

O'Brien WD Jr., Zachary JF. Lung damage assessment from exposure to pulsed-wave ultrasound in the rabbit, mouse and pig. IEEE Trans Ultrason Ferroelectr Freq Control 1997;44:473–485.

O'Brien WD Jr., Simpson DG, Frizzell LA, Zachary JF. Superthreshold behavior and threshold estimation of ultrasound-induced lung hemorrhage in adult rats: Role of beamwidth. IEEE Trans Ultrason Ferroelectr Freq Control 2001;48:1695–1705.

O'Brien WD Jr., Simpson DG, Frizzell LA, Zachary JF. Threshold estimates and superthreshold behavior of ultrasound-induced lung hemorrhage in adult rats: Role of pulse duration. Ultrasound Med Biol 2003b;29:1625–1634.

O'Brien WD Jr., Simpson DG, Ho M-H, Miller RJ, Frizzell LA, Zachary JF. Superthreshold behavior and threshold estimation of ultrasound-induced lung hemorrhage in pigs: Role of age dependency. IEEE Trans Ultrason Ferroelectr Freq Control 2003a;50:153–169.

O'Brien WD Jr., Simpson, DG, Frizzell, LA, Zachary, JF. Superthreshold behavior of ultrasound-induced lung hemorrhage in adult rats: Role of pulse repetition frequency and pulse duration. J Ultrasound Med 2006;25:873–882.

ODS, Standard for Real-Time Display of Thermal and Mechanical Acoustic Output Indices on Diagnostic Ultrasound Equipment, Rev. 1. Laurel, MD, American Institute of Ultrasound in Medicine, and Rosslyn, VA, National Electrical Manufacturers Association, 1998.

Raum K, O'Brien WD Jr. Pulse-echo field distribution measurement technique of high-frequency ultrasound sources. IEEE Trans Ultrason Ferroelectr Freq Control 1997;44:810–815.

Sempsrott JM, O'Brien WD Jr. Experimental verification of acoustic saturation. Proc IEEE Ultrason Symp 1999:1287–1290.

Simpson, DG, Ho, M, Yang, Y, Zhou, J, Zachary, JF, O'Brien WD Jr. Excess risk thresholds in ultrasound safety studies: Statistical methods for data on occurrence and size of lesions. Ultrasound Med Biol 2004;30:1289–1295.

Tarantal AF, Canfield DR. Ultrasound-induced lung hemorrhage in the monkey. Ultrasound Med Biol 1994;20:65–72.

Teotico GA, Miller RJ, Frizzell LA, Zachary JF, O'Brien WD Jr. Attenuation coefficient estimates of mouse and rat chest wall. IEEE Trans Ultrason Ferroelectr Freq Control 2001;48:593–601.

Towa RT, Miller RJ, Frizzell LA, Zachary JF, O'Brien WD Jr. Attenuation coefficient and propagation speed estimates of rat and pig intercostal tissue as a function of temperature. IEEE Trans Ultrason Ferroelectr Freq Control 2002;49:1411–1420.

Zachary JF, Sempsrott JM, Frizzell LA, Simpson DG, O'Brien WD Jr. Superthreshold behavior and threshold estimation of ultrasound-induced lung hemorrhage in adult mice and rats. IEEE Trans Ultrason Ferroelectr Freq Control 2001;48:581–592.